

THE PHYSICAL REVIEW

A journal of experimental and theoretical physics established by E. L. Nichols in 1893

SECOND SERIES, VOL. 184, No. 1

5 AUGUST 1969

Analytic Independent-Particle Model for Atoms*

Alex E. S. Green, D. L. Sellin, and A. S. Zachor[†]

Department of Physics and Astronomy, University of Florida, Gainesville, Florida 32601

(Received 14 April 1969)

A simple analytic electron-atom independent-particle model (IPM) potential for use in phenomenological studies is examined. The potential is given by $V(r) = 2(N_T - Z)/r$, $T = 1 - [(e^{r/d} - 1)H + 1]^{-1}$, where Z is the number of nuclear protons, N the number of core electrons, and Rydberg units are used. The adjustable parameters d and H are evaluated using (1) Thomas-Fermi screening functions, (2) Herman and Skillman Hartree-Fock-Slater (HS-HFS) screening functions, (3) HS-HFS eigenvalues, (4) Hartree-Fock eigenvalues, and (5) experimental separation energies. Good agreements with HS-HFS eigenvalues and screening functions for electrons in neutral atoms is obtained if $H = d\alpha N^{0.4}$, where d is adjusted for each element and $\alpha = 1.05$ for HFS and 1.00 for HF models. The success in fitting energy values and screening functions suggests that the potential embodies exchange and possibly correlation effects. Applications of the model to excited states and elastic and inelastic collisions are discussed.

1. INTRODUCTION

The nuclear independent-particle model¹ (IPM), based upon phenomenological analytic shell and optical-model potentials, has contributed greatly to the development of techniques for calculating nuclear elastic and inelastic scattering cross sections, transition probabilities, and other important properties. An analytic atomic IPM, which maintains a close relationship to fundamental theoretical models, could also be useful to applied atomic physics for the approximate calculation of analogous atomic properties. Motivated by this need, the present study takes as a starting point an approximate analytical characterization of the universal Thomas-Fermi potential.^{2,3}

2. ANALYTIC REPRESENTATIONS OF THE THOMAS-FERMI POTENTIAL

In the IPM approximation, the radial Schrödinger equation for one-electron orbitals of angular momentum l and principal quantum number n is

$$\left(\frac{d^2}{dr^2} - \frac{l(l+1)}{r^2} - V(r) + E_{nl} \right) P_{nl}(r) = 0, \quad (1)$$

where r has units of Bohr radii (a_0), and all energies are in Ry. Here, E_{nl} is the eigenvalue, and $V(r)$ is a central atomic potential due to the Z units of nuclear charge and the average effect of the N remaining core electrons.

Analytic representations of atomic potentials

have already been proposed. Almost all such attempts have made use of analytic approximations to the potential derived from the statistical model of Thomas and Fermi^{2,3} (TF). In the simplest form of this theory, the potential energy of a single electron in a neutral atom is taken as

$$V(r) = -2Z\phi_{\text{TF}}(x)/r, \quad (2)$$

where the screening function $\phi_{\text{TF}}(x)$ satisfies the dimensionless TF equation

$$x^{1/2}(d^2\phi_{\text{TF}}/dx^2) = \phi_{\text{TF}}^{3/2}, \quad (3)$$

where $x = rZ^{1/3}/\mu_0$, $\mu_0 = \frac{1}{2}(\frac{3}{4}\pi)^{2/3} = 0.8853$. In the usual elementary treatment, the screening function ϕ is assumed to satisfy $\phi_{\text{TF}}(0) = 1$ and $\phi_{\text{TF}}(x) \rightarrow 0$ as $x \rightarrow \infty$. These equations were first solved by Bush and Caldwell⁴ with a differential analyzer. The points in Fig. 1 are interpolated from their numerical values.

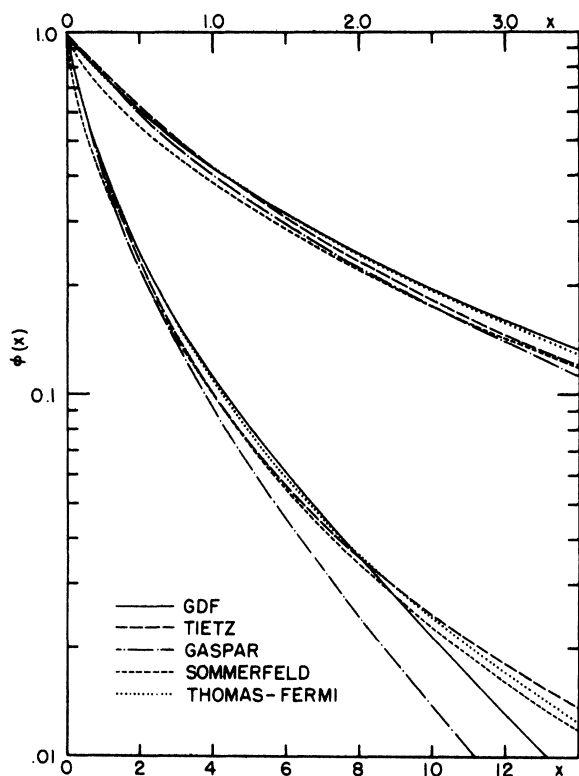


FIG. 1. Comparison of analytic representations of the TF screening function. The TF function (Ref. 4) appears as dots; the legend for various analytic representations are indicated in the diagram. The expanded horizontal scale at the top of the figure refers to the upper curves. (x is in a.u.)

Several analytic forms have appeared in the literature which fit the numerical output of Bush and Caldwell to various degrees of approximation. Sommerfeld⁵ has used

$$\phi_s(x) = [1 + x/(12)^{2/3}]^{-3.885}. \quad (4)$$

More recently, Gaspar⁶ employed the form

$$\phi_g(x) = e^{-0.1837x/(1+1.05x)}, \quad (5)$$

while Teitz⁷ has suggested

$$\phi_t(x) = [1 + (\frac{1}{8}\pi)^{2/3}x]^{-2}. \quad (6)$$

Figure 1 also gives these three functions.

Latter⁸ has given a very precise (0.3%) fit to ϕ_{TF}^{-1} in the form of a polynomial of the sixth degree in $x^{1/2}$. However, his use of six parameters is unnecessarily cumbersome for the applications which we envisage.

The shape of the $\phi_{\text{TF}}(x)$ on semilog paper suggested to us that a generalized distribution function (GDF)⁹ is of the form

$$\phi_{\text{GDF}}(x) = (1 + \beta)/(e^{x/\delta} + \beta). \quad (7)$$

Such a function has proved useful in representing atmospheric density distributions when departures from a simple exponential falloff ($\beta = 0$) occur at small values of x . This function contains a special case the Fermi-Dirac function ($\beta > 0$) (which is mathematically the same as Woods-Saxon IPM potential of nuclear physics), the Maxwell-Boltzmann function ($\beta = 0$), and the Einstein-Bose function ($\beta \rightarrow -1$).

For our purposes here, we reparametrize this function using $H = (1 + \beta)^{-1}$, in which case

$$\phi_{\text{GDF}}(x) = [H(e^{x/\delta} - 1) + 1]^{-1}. \quad (8)$$

The solid line in Fig. 1 represents this function for the parameter values $\delta = 4.478$ and $H = \delta + 1$. It is clear that the GDF function achieves the best fit to the TF function in the region $x = 0-8$, which is the major range of interest. The rapid falloff of the GDF function beyond $x = 8$ poses no problem in our applications - indeed for some purposes it is an asset. A minor improvement in the fit may be obtained if the shape factor H and the scaling factor δ are adjusted independently.

Latter has discussed the problem of the asymptotic behavior of the TF and Thomas-Fermi-Dirac (TFD) potentials. Because of this problem, it is customary to use a TF or TFD potential only out to the radius r_0 at which it equals $V_h = -2/r$, and to use $V = V_h$ for $r > r_0$. Effectively, one uses the screening function ϕ_{TF} only for $x < x_0 = r_0 Z^{1/3}/\mu_0$

and uses $\phi(x) = Z^{-1}$ at $x > x_0$. In the present work, we wished to avoid this *ad hoc* device, which introduces a discontinuity in the derivative of the potential at r_0 . We do this by writing the potential for an electron in a neutral atom in the form

$$V(r) = -2r^{-1}[(Z-1)\Omega(r) + 1], \quad (9)$$

where from $\phi_{\text{TF}}(x)$, we evaluate

$$\Omega_{\text{TF}}(x, Z) = [\phi_{\text{TF}}(x) - Z^{-1}] / (1 - Z^{-1}). \quad (10)$$

We fit $\Omega_{\text{TF}}(x, Z)$ by the GDF function, using x as the independent variable. Fits for a sample of elements from $Z = 5$ to 100 showed a rather unexpected behavior in the parameters δ and H : Instead of these parameters remaining approximately constant, they varied approximately as $Z^{1/3}$. This first observation suggested that we use the radial coordinate r rather than the scaled radial coordinate x . Accordingly, for further discussions, we parametrize our modified screening function in the form

$$\Omega(r) = [H(e^{r/d} - 1) + 1]^{-1}, \quad (11)$$

where d is approximately the same for all elements; Fig. 2 shows screening function shapes for various H .

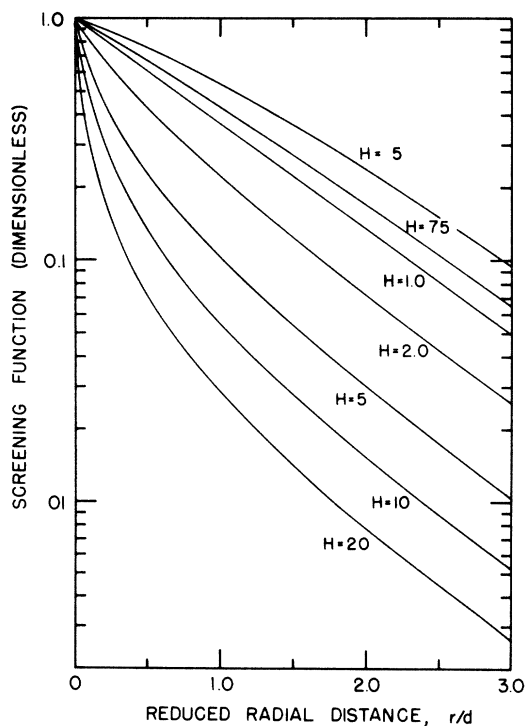


FIG. 2. Shapes of screening functions corresponding to various H ($d = 1$).

Energy eigenvalues were calculated with such a potential with $d = 0.57$ and $H = 0.72Z^{1/3}$ using the eigenvalue subprogram of the Herman and Skillman HFS¹⁰ computer code. The energies were as accurate as those of Latter. However, it became clear in the course of the study that local changes in d and H could greatly improve the eigenvalues.

Previously, Stewart and Rotenberg¹¹ have noted that by scaling the radial coordinate of numerically generated TF potentials differently for each state, they could greatly improve the accuracy of the eigenvalues and wave functions obtained from it. The present analytic framework provides a far simpler procedure for doing this and should achieve comparable results. We may also adjust d and H to a HF calculation such as carried out by Mann.¹²

Let us first consider the application to the HFS approximation, i. e., in which an approximate exchange correction is applied based upon the free-electron gas theory.¹³

3. ANALYTIC FITS OF HFS SCREENING FUNCTIONS

HFS self-consistent field calculations have been carried out by Herman and Skillman¹⁰ (HS) for neutral atoms for $Z = 2-103$. They express their one-electron potential energy in terms of a "normalized" potential U , which is the same as our ϕ in Eq. (2). These were transformed to modified screening functions $\Omega_{\text{HS}}(r)$ using Eq. (10). For each Z , values of the parameters H and d were obtained by a least-squares fit of the GDF function [Eq. (11)] to $\Omega_{\text{HS}}(r)$. The values of the d 's obtained fluctuated markedly around 0.8. The resulting values of H tended generally to increase as a function of $N = Z - 1$ but displayed local correlations with the fluctuations in d . Empirically it was found convenient to express H in the form

$$H = d\alpha N^\nu, \quad (12)$$

where, when ν was fixed at 0.4, the parameter α was found to be approximately 1.05 for all elements. Using this relationship, least-squares fits were made to obtain new values of d . This one-parameter description of the HFS screening function proved to be nearly as accurate as the one obtained by varying both H and d . Figure 3 illustrates several fits to $\Omega_{\text{HS}}(r)$ obtained in our studies.

Having obtained the parameters for the analytic IPM potentials, the eigenvalues were obtained for a sample of elements. Good eigenvalues in relation to the HS-HFS eigenvalues were obtained for both the two-parameter and one-parameter descriptions. The latter sets were somewhat better, suggesting that the asymptotic behavior of these screening functions were, fortuitously, somewhat better.

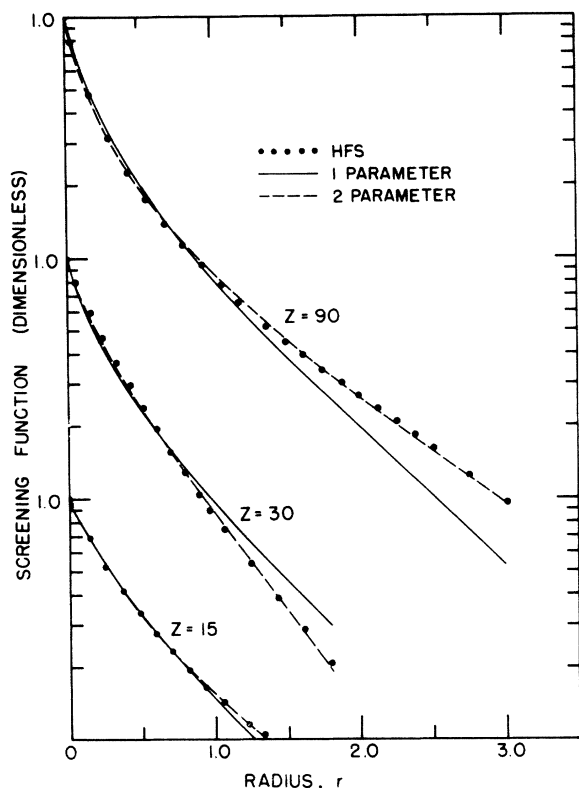


FIG. 3. Representative fits to modified HFS screening functions. The dots give the modified HFS screening functions. The one-parameter least-square fits are shown as a solid line; the two-parameter results (varying H and d) are shown by the broken line. (r is in a.u.)

4. EIGENVALUES

A. Adjustment of IPM Potential Parameters Using Eigenvalues

As might have been expected, we found that agreement between our IPM eigenvalues E_j and

the HS eigenvalues E_j (HS-HFS) could be improved further by determining d and α from the E_j (HS-HFS) rather than from the $\Omega_{\text{HF}}(r)$. Thus, we revised our original estimates of d and α by a formal least-squares procedure, minimizing the sum

$$\chi^2 = \sum_j [E_j(\text{HS-HFS}) - E_j]^2 / E_j(\text{HS-HFS}). \quad (13)$$

Table I gives some representative comparisons of d and α obtained from the modified screening function and from the eigenvalues.

B. Adjustment to HF Energies

Using the same weighted least-squares method and the same starting values, we obtained new values for d and α by fitting the energies computed by Mann¹² from the coupled HF equations. This is an interesting case, since exchange is represented exactly in the HF equations. Thus, the IPM potential for the d 's and α 's determined from the Mann-Hartree-Fock (MHF) energies includes an "average" exchange potential. Since the exchange potential embodied in the HS calculations is now recognized to require modification,^{14,15} we have concentrated our attention on finding an IPM simulation of MHF calculations.

By adjusting to MHF energies, we computed a complete set of d 's and α 's for helium through lawrencium. After these calculations were completed, we found that setting $\alpha = 1$ caused no significant loss of accuracy in the fits to the eigenvalues. Table II presents the values of d for the best analytic potentials so obtained. Column 5 of Table III gives a sample set of energies computed from our analytic potential and the parameter values of Table II. Column 4 gives the corresponding MHF energies. Column 3 gives HS-HFS energies. It should be noted that the differences between our computed energies and the MHF energies are generally much smaller than the dif-

TABLE I. Comparison of various d and α values obtained by fitting HFS screening functions, HFS eigenvalues, and HF (Mann) eigenvalues.

Z	d^a	d^b	α^b	d^c	α^c	d^d
5	0.877	0.977	1.120	0.780	1.02	0.979
10	0.466	0.443	0.997	0.466	1.04	0.500
15	0.920	1.060	1.140	0.919	1.08	0.867
20	1.140	1.080	1.010	1.170	1.05	1.154
30	0.593	0.559	1.000	0.598	1.02	0.612
40	0.951	1.010	1.090	0.942	1.06	0.866
50	0.846	0.789	1.000	0.841	1.03	0.841
70	0.725	0.752	1.090	0.632	1.00	0.654
90	1.060	1.090	1.080	0.924	1.02	0.927

^aFit of d to HFS screening functions with $\alpha = 1.05$.

^cFits of d and α to HFS eigenvalues.

^bFits of d and α to HFS screening functions.

^dFit of d to HF (Mann) eigenvalues with $\alpha = 1.00$.

TABLE II. Values of d to fit HF energies ($\alpha = 1.00$). Note for $Z=1$ (H), d is indeterminate; for $Z=2$ (He), $d=0.215$.

Z	Symbol	d	Z	Symbol	d
II			III		
3	Li	0.563	11	Na	0.561
4	Be	0.858	12	Mg	0.621
5	B	0.979	13	Al	0.729
6	C	0.880	14	Si	0.817
7	N	0.776	15	P	0.868
8	O	0.708	16	S	0.885
9	F	0.575	17	Cl	0.881
10	Ne	0.500	18	A	0.862
IV			V		
19	K	1.006	37	Rb	0.744
20	Ca	1.154	38	Sr	0.798
21	Sc	1.116	39	Y	0.855
22	Ti	1.060	40	Zr	0.866
23	V	0.996	41	Cb	0.831
24	Cr	0.837	42	Mo	0.825
25	Mn	0.866	43	Tc	0.855
26	Fe	0.807	44	Ru	0.803
27	Co	0.751	45	Rh	0.788
28	Ni	0.700	46	Pd	0.737
29	Cu	0.606	47	Ag	0.754
30	Zn	0.612	48	Cd	0.775
31	Ga	0.631	49	In	0.810
32	Ge	0.649	50	Sn	0.841
33	As	0.663	51	Sb	0.870
34	Se	0.675	52	Te	0.896
35	Br	0.684	53	I	0.919
36	Kr	0.689	54	Xe	0.940

ferences between the HS-HFS and MHF energies. Columns 6 and 7 give the derivative of the energy with respect to parameters d and α .

C. Experimental Energies

In addition to obtaining values of d and α , which give good agreement with the HF energies, attempts were made to find values of d and α that give the experimental ionization (ESCA)¹⁶ potentials for selected elements. These experimental energies were first averaged to eliminate spin-orbit splitting. For $Z \leq 40$, α and d values were readily found that provided reasonable agreement. However, for $Z \geq 50$, relativistic effects became appreciable. That these effects cannot be accounted for in the present nonrelativistic framework, is best seen by considering, as an example, thorium ($Z=90$). The experimental binding energy of a 1s electron is 8060 Ry, the corresponding HF energy is 7102 Ry, and the unscreened

TABLE II. (continued)

Z	Symbol	d	Z	Symbol	d
VI			VII		
55	Cs	1.022	87	Fr	0.818
56	Ba	1.108	88	Ra	0.859
57	La	1.150	89	Ac	0.899
58	Ce	1.081	90	Th	0.927
59	Pr	0.970	91	Pa	0.887
60	Nd	0.938	92	U	0.880
61	Pm	0.905	93	Np	0.872
62	Sm	0.873	94	Pu	0.832
63	Eu	0.842	95	Am	0.822
64	Gd	0.862	96	Cm	0.842
65	Tb	0.830	97	Bk	0.830
66	Dy	0.754	98	Cf	0.790
67	Ho	0.728	99	Es	0.778
68	Er	0.702	100	Fm	0.766
69	Tm	0.677	101	Mv	0.754
70	Yb	0.654	102	No	0.742
71	Lu	0.665	103	Lw	0.755
72	Hf	0.672			
73	Ta	0.676			
74	W	0.679			
75	Re	0.680			
VI					
76	Os	0.680			
77	Ir	0.679			
78	Pt	0.661			
79	Au	0.657			
80	Hg	0.671			
81	Tl	0.690			
82	Pb	0.708			
83	Bi	0.726			
84	Po	0.744			
85	At	0.761			
86	Rn	0.777			

(hydrogenlike) nonrelativistic energy is 8100 Ry. Since the form of the potential automatically provides for some screening, it is not surprising that so large a binding energy cannot be obtained for any reasonable set of screening parameters.

As an alternative approach, the relativistic effects tabulated by HS were subtracted from the experimental energies for a sample of elements with $Z \geq 40$. Then values of d and α , similar to those obtained from HFS and HF energies, were found to give energies in reasonable agreement with those obtained from the experimental data. This agreement, however, deteriorates somewhat for very heavy elements. The experimental ESCA values averaged over the spin-orbit effect and corrected for the relativistic terms of HS are given in column 2 of Table III.

TABLE III. Comparison of Energies for $Z=10, 20, 30, 40, 50, 70$, and 90 .

Shell	ESCA	HFS	HF	IPM	dE/dd	$dE/d\alpha$
$Z=10, d=0.500, H=1.203$						
1s	63.70	62.99	65.54	64.24	7.20	-25.90
2s	3.30	3.17	3.86	3.54	6.03	-4.66
2p	1.30	1.47	1.70	1.88	6.22	-5.02
$Z=20, d=1.154, H=3.747$						
1s	296.80	293.50	298.70	297.40	4.68	-80.30
2s	32.20	31.63	33.65	33.06	3.42	-30.90
2p	25.70	26.18	27.26	28.10	3.48	-35.20
3s	3.20	3.88	4.49	4.09	2.07	-6.97
3p	1.90	2.48	2.68	2.72	1.97	-6.60
4s	...	0.40	0.39	0.49	0.44	-0.73
$Z=30, d=0.612, H=2.352$						
1s	710.00	698.40	706.60	705.60	9.85	-163
2s	87.80	85.12	88.72	86.35	19.00	-72.3
2p	76.20	75.55	77.85	77.53	18.60	-82.0
3s	10.10	9.79	11.28	10.50	13.20	-18.8
3p	6.40	6.66	7.68	7.40	13.00	-19.0
3d	0.70	1.26	1.57	1.76	12.20	-15.6
4s	...	0.62	0.59	0.72	2.09	-1.45
$Z=40, d=0.866, H=3.748$						
1s	1290.00	1291.00	1301.00	1303.00	6.97	-251.0
2s	177.60	178.00	182.80	182.90	12.10	-127.0
2p	164.00	163.80	167.00	169.80	11.90	-143.0
3s	30.00	29.80	32.12	31.97	11.10	-45.0
3p	24.30	24.36	26.05	26.68	11.10	-47.2
3d	13.20	14.32	15.05	16.58	11.40	-49.2
4s	3.60	4.23	4.85	4.35	5.50	-10.5
4p	2.00	2.73	2.99	2.80	4.97	-9.24
4d	...	0.52	0.62	0.47	3.08	-4.43
5s	...	0.44	0.42	0.44	0.76	-0.85
$Z=50, d=0.841, H=3.991$						
1s	2065.00	2069.00	2082.00	2085.00	7.42	-363.0
2s	307.70	307.80	314.00	313.00	18.00	-195.0
2p	290.90	288.80	293.00	295.60	16.20	-218.0
3s	60.40	60.07	63.21	61.52	15.50	-77.7
3p	52.40	52.09	54.43	53.79	15.60	-82.2
3d	35.40	37.16	38.34	38.77	16.20	-89.0
4s	9.10	9.76	11.03	10.34	9.35	-22.6
4p	6.07	7.06	7.95	7.66	9.13	-21.5
4d	1.68	2.53	2.75	3.03	8.02	-17.0
5s	...	0.92	0.96	1.07	2.59	-3.25
5p	...	0.44	0.50	0.53	1.70	-1.97
$Z=70, d=0.654, H=3.557$						
1s	4195.00	4190.00	4209.00	4216.00	14.2	-613.00
2s	682.30	682.90	692.00	686.50	34.2	-364.00
2p	671.20	554.00	660.40	660.50	32.0	-403.00
3s	153.90	153.40	158.40	152.60	38.2	-166.00
3p	143.70	140.00	143.90	139.50	38.4	-177.00
3d	111.40	114.70	117.20	113.40	39.5	-197.00

TABLE III. (continued)

Shell	ESCA	HFS	HF	IPM	dE/dd	$dE/d\alpha$
$Z=70, d=0.654, H=3.557$						
4s	30.30	29.59	32.19	30.79	27.7	-58.90
4p	25.20	24.07	26.17	25.33	27.4	-58.90
4d	13.40	14.01	15.32	15.11	26.8	-56.00
4f	3.10	1.18	1.47	1.94	24.2	-40.50
5s	1.40	3.74	4.20	3.85	11.4	-12.80
5p	...	2.26	2.41	2.27	9.75	-10.50
6s	...	0.38	0.36	0.35	0.77	-0.62
$Z=90, d=0.927, H=5.580$						
1s	7066.00	7078.00	7102.00	7116.00	6.94	-893.00
2s	1253.00	1227.00	1239.00	1235.00	23.7	-559.00
2p	1258.00	1188.00	1196.00	1200.00	19.4	-617.00
3s	313.80	308.50	315.00	311.80	25.2	-286.00
3p	302.80	289.10	294.20	292.70	24.4	-305.00
3d	241.70	252.50	255.80	255.00	26.1	-338.00
4s	79.00	77.75	81.46	81.38	20.9	-124.00
4p	71.70	68.78	71.84	72.52	21.0	-126.00
4d	48.40	51.99	54.06	55.51	21.0	-129.00
4f	24.20	28.70	29.43	31.91	21.9	-125.00
5s	16.50	17.45	18.94	18.54	13.2	-43.50
5p	13.50	14.00	15.09	15.02	12.9	-41.80
5d	6.15	7.97	8.283	8.71	12.0	-36.30
6s	3.42	2.98	3.386	2.90	5.65	-10.50
6p	3.05	1.97	2.135	1.85	4.85	-8.56
6d	...	0.52	0.592	0.38	2.51	-3.52
7s	...	0.36	0.342	0.34	0.67	-0.86

5. SCALING PARAMETER AND RADIAL ELECTRON DENSITIES

Figure 4 gives the value d obtained by fitting Mann's energies with α fixed at 1.00. One sees only a loose correlation between the minima of d and the magic numbers. It would appear that d , which in this parametrization influences both the scale and shape of the potential, is strongly affected by the middle electrons as well as by the outer electrons.

Here it must be recognized that the electrostatic potential arising from a charge density is rather effectively "filtered" out of the radially fluctuating components in the density. This is apparent, for example, in the smooth nature of the HS-HFS screening functions illustrated in Fig. 3. Accordingly, two very similar potentials can arise from fairly different charge densities. The wave functions and eigenvalues are, of course, responsive to the potential rather than the density function.

It is constructive to write our analytic potential in the form

$$V = V_e + V_n = 2r^{-1} [N\Upsilon - Z], \quad (14)$$

where V_n is the nuclear potential, and V_e is the potential energy due to the electronic cloud. The function

$$\Upsilon(r) = 1 - \Omega(r) = HT(HT+1)^{-1}, \quad (15)$$

where $T = (e^\xi - 1)$ and $\xi = r/d$. To obtain the electronic part of the radial probability density $4\pi r^2 \rho(r)$, we have, from Poisson's equation

$$\begin{aligned} 4\pi r^2 \rho(r) &= -r^2 \nabla^2 [N\Upsilon(r)/r] \\ &= (N/d) \xi [He^\xi / (HT+1)^2] [-1 + 2He^\xi / (HT+1)]. \end{aligned} \quad (16)$$

Figure 5 gives a plot of the radial probability density divided by N/d as a function of $\xi = r/d$. This scaling is used to obtain clarity in the face of the irregularities of d . We see that the increasing H corresponds to increasing the inner concentration of the electronic cloud.

6. CONCLUSION

A simple analytic atomic IPM potential with a

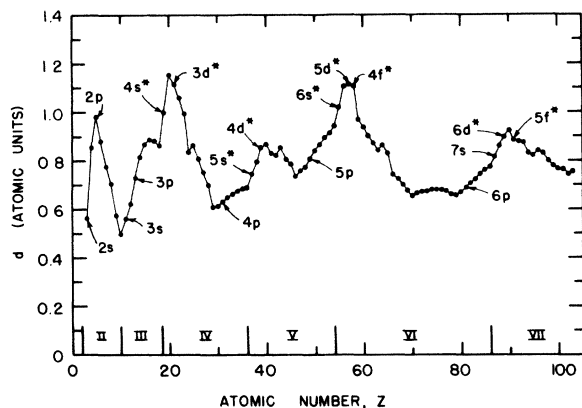


FIG. 4. Graph of the optimum values of d that were obtained by fitting Mann's HF energies with $\alpha = 1.0$. Symbols denote filling orbitals (*competitive).

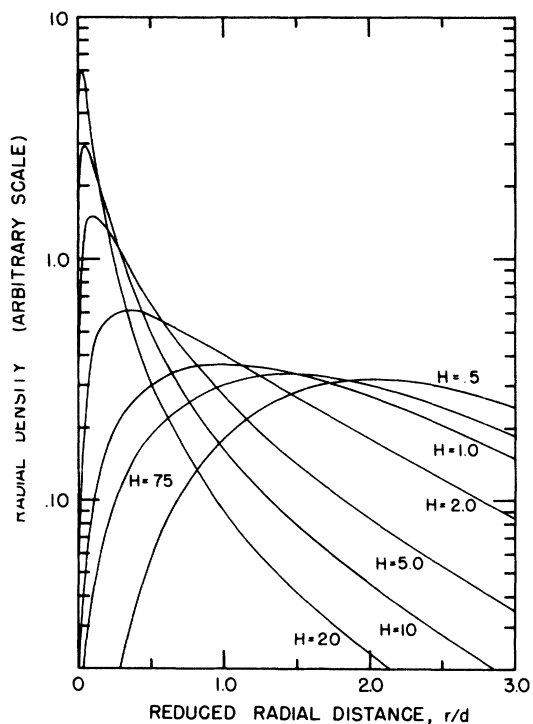


FIG. 5. Normalized radial probability distribution various values of H . The vertical scaling factor N/d is set equal to unity.

continuous first derivative has been found, which uses only two parameters. With one parameter (α) established for the entire Periodic Table and one parameter (d) adjusted for each element, we can fit all bound-state energies within a few percent. The fact that these IPM energies also agree approximately with the experimental removal energies confirms the approximate validity of Koop-

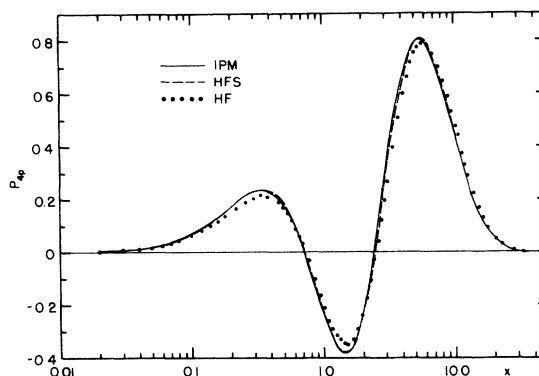


FIG. 6. Wave functions for the $4p$ state of argon. (x is in a.u.)

mans's¹⁷ theorem for atoms. For the outermost states, somewhat greater departures occur, but one must recognize here that multiplet splittings are proportionally larger and more varied for such states.

Figure 6 shows a radial wave function for the $4p$ state of Ar based upon our IPM potential. It is shown in comparison with the HF wave function of Mann and the HFS wave function of HS. The close similarity of all three wave functions is encouraging. The scaled TF wave function of Stewart and Rotenberg, which involves a much more complex calculation, is practically the same as our IPM wave function.

Since our IPM central potential is common to all the electrons in an atom, it provides a complete and orthogonal basis set which should be helpful for study of residual perturbations. For some purposes it might be desirable to adjust the parameters d and α for each l value, which would permit greater precision yet still preserve the orthogonality property. This in effect, would build in nonlocality, which may be a simple way to approximate remaining exchange and correlation effects. One can also deal with the spin-orbit splitting in a similar way. A table of eigenvalues and eigenvalue derivatives may be used for this purpose.¹⁸

In view of our success with the bound states of neutral atoms and the apparent versatility of our analytic form for \mathcal{T} , it is not unreasonable to hope that Eq. (14) might, with minor adjustments in d and α , be applicable to ions as well.

For excited states, a polarization potential would probably be needed. We have found a number of simple analytic potentials which fit our analytic potential in the range $r=0-2$ (a_0) which go over asymptotically to $Pr^{-4} + 2r^{-1}$, where P is the dipole polarizability. Excited-state energies using these potentials are under study.

For scattering calculations, an imaginary potential will also be needed (as in the nuclear optical model). In addition, dynamical polarization and exchange terms such as those studied for the case of e -He scattering by Callaway *et al.*,¹⁹ also arise whose magnitudes might be established phenomenologically. It is reasonable to hope that an analytic IPM optical potential along these lines could be useful for the calculation of approximate elastic and inelastic electron impact cross sections

which are needed in applications.

ACKNOWLEDGMENTS

The authors would like to express their thanks to Professor John C. Slater for his helpful suggestions, Dr. T. Wilson and Dr. J. Conklin for their assistance with the HS program, and Dr. J. E. Purcell, Professor Hugh Kelly, and Dr. Frank Herman for useful discussions.

*Supported in part by U. S. Atomic Energy Commission Grant No. AEC-AT-(40-1)-3798.

†Present address: Honeywell Radiation Center, 2 Forbes Road, Lexington, Mass. 02173.

¹A. E. S. Green, T. Sawada, and D. S. Saxon, The Nuclear Independent-Particle Model (Academic Press Inc., New York, 1968), e.g., for a recent summary of work on the Nuclear IPM.

²L. H. Thomas, Proc. Cambridge Phil. Soc. 23, 542 (1927).

³E. Fermi, Z. Physik 48, 73 (1928).

⁴V. Bush and S. H. Caldwell, Phys. Rev. 38, 1898 (1931).

⁵A. Sommerfeld, Rend. Accad. Lincei 6, 15 (1932); 6, 788 (1932).

⁶R. Gaspar, Acta Phys. Hung. II, 151 (1952).

⁷Von T. Teitz, Ann. Physik 15, 186 (1955).

⁸R. Latter, Phys. Rev. 99, 510 (1955).

⁹A. E. S. Green and P. J. Wyatt, Atomic and Space Physics (Addison Wesley Publishing Co., Inc., Reading, Mass., 1965), p. 445.

¹⁰F. Herman and S. Skillman, Atomic Structure Calculations (Prentice-Hall, Inc., Englewood Cliffs, N. J., 1963).

¹¹J. C. Stewart and M. Rotenberg, Phys. Rev. A140, 1508 (1965).

¹²J. B. Mann, Los Alamos Scientific Laboratory, Report No. LA-3690 1968.

¹³John C. Slater, Quantum Theory of Matter (McGraw-Hill Book Co., New York, 1968), 2nd ed.

¹⁴W. Kohn and L. J. Sham, Phys. Rev. 140, A1133 (1965).

¹⁵D. A. Liberman, Phys. Rev. 171, 1 (1968).

¹⁶K. Siegbahn, *et al.*, ESCA Atomic Molecular and Solid State Structure Studied by Means of Electron Spectroscopy (Almqvist-Wiksells Bokh, A. B. Uppsala, 1967).

¹⁷T. A. Koopmans, Physica 1, 104 (1933).

¹⁸Tables of eigenvalues and eigenvalue derivatives are available upon request.

¹⁹J. Callaway, R. W. LaBahn, R. T. Pu, and W. M. Duxler, Phys. Rev. 168, 12 (1968).